

## Electronic Supplementary Information (ESI)

for

### **Cobalt oxide 2D nano-assemblies from infinite coordination polymer precursor mediated by multidentate pyridyl ligand**

Guo-Rong Li<sup>a,c</sup>, Chen-Chao Xie<sup>a,c</sup>, Zhu-Rui Shen<sup>\*b</sup>, Ze Chang<sup>\* a,c</sup>, and Xian-He Bu<sup>a,c</sup>

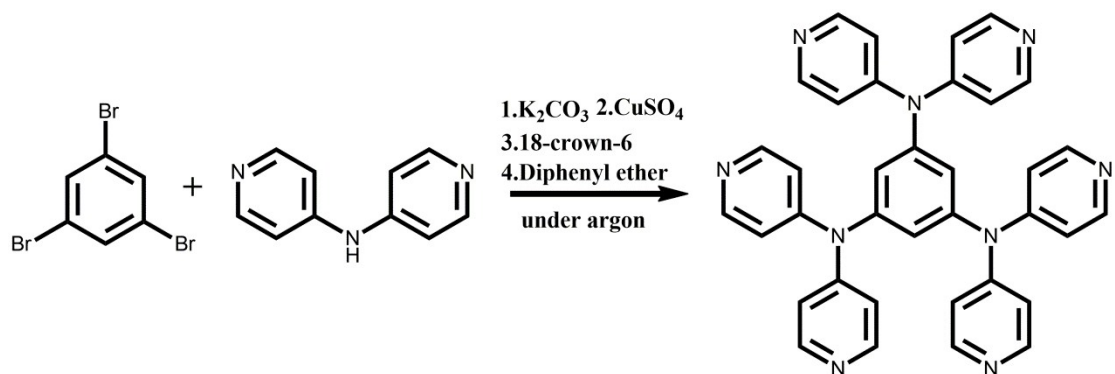
*a. School of Materials Science and Engineering, National Institute for Advanced Materials, Nankai University, Tianjin 300350, P. R. China.*

*b. Key Laboratory for Advanced Ceramics and Machining Technology of Ministry of Education & School of Material Science and Engineering, Tianjin University, Tianjin 300072, P. R. China.*

*c. Collaborative Innovation Center of Chemical Science and Engineering (Tianjin), Nankai University, Tianjin 300071, P. R. China.*

Corresponding author Email: [changze@nankai.edu.cn](mailto:changze@nankai.edu.cn), [shenzhurui@tju.edu.cn](mailto:shenzhurui@tju.edu.cn)

## Section 1 The characterization of Hppd.



Scheme S1 Synthetic route of Hppd.

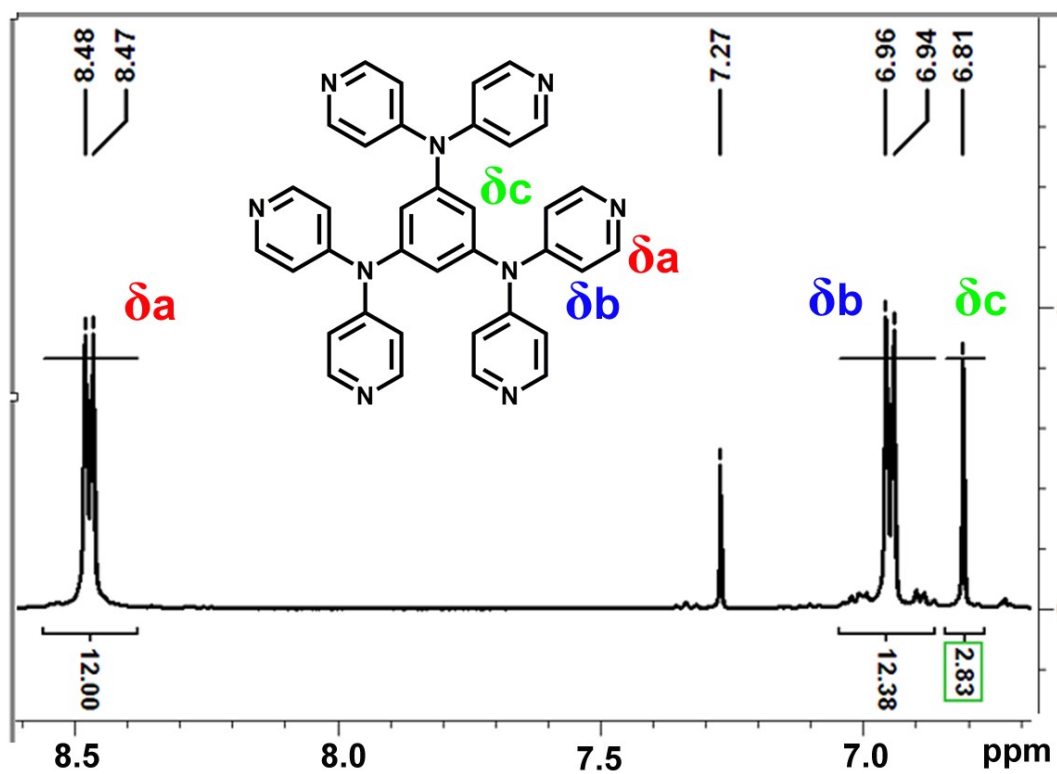


Fig. S1 The  $^1H$  NMR of Hppd.

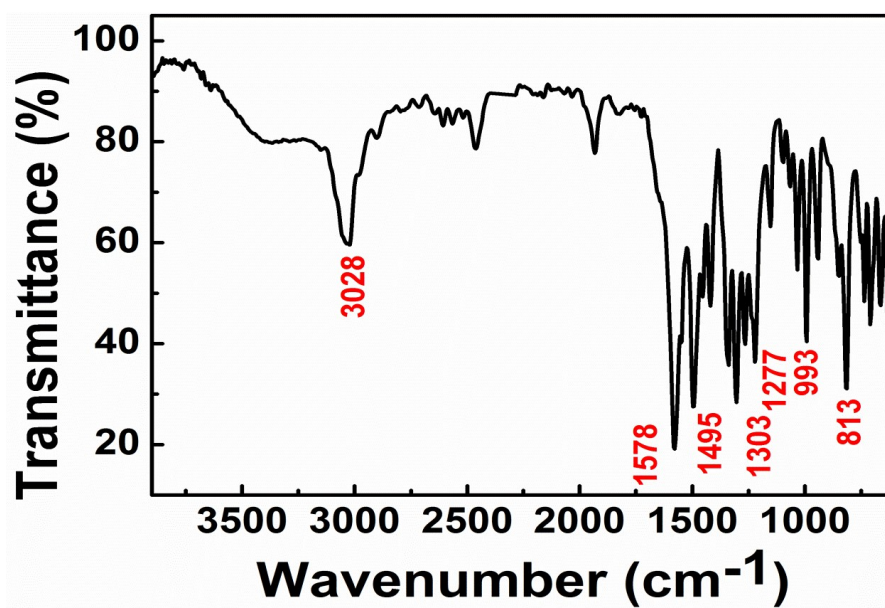
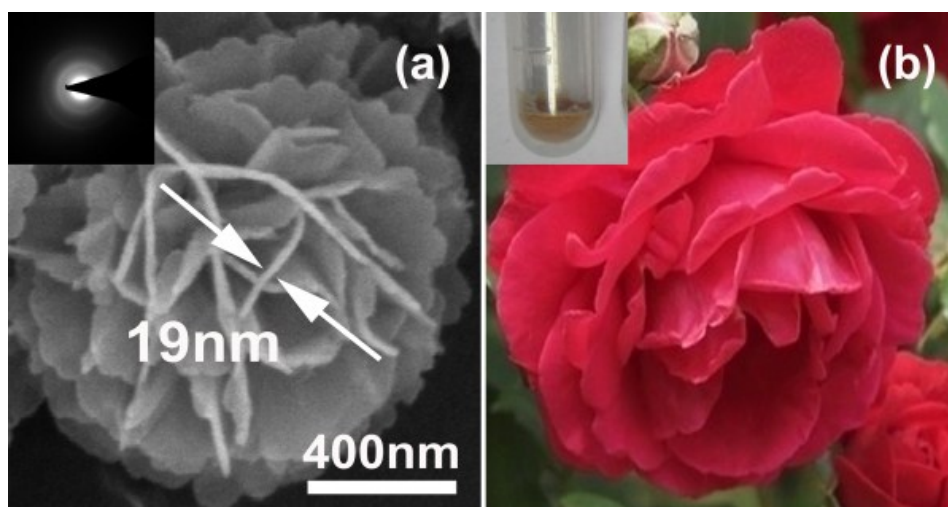


Fig. S2 The IR spectrum of Hppd.

Table S1. The EA analysis result of Hppd.

Type \ Value	C	N	H
Calculation(%)	73.83	21.52	4.65
Experiment(%)	73.69	21.6	4.71

## Section 2. The complementary characterization of Co 2D-ICPP.



**Fig. S3** (a) The SEM and SAED (inset) images of Co 2D-ICPP, (b) The picture of nature flower and optical photograph of Co 2D-ICPP.

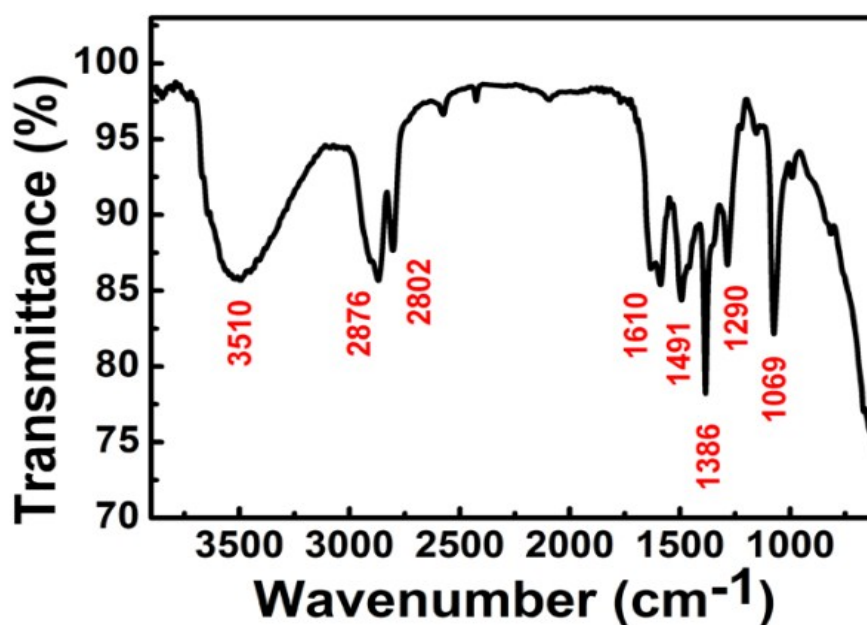


**Fig. S4** The IR spectrum of Co 2D-ICPP.

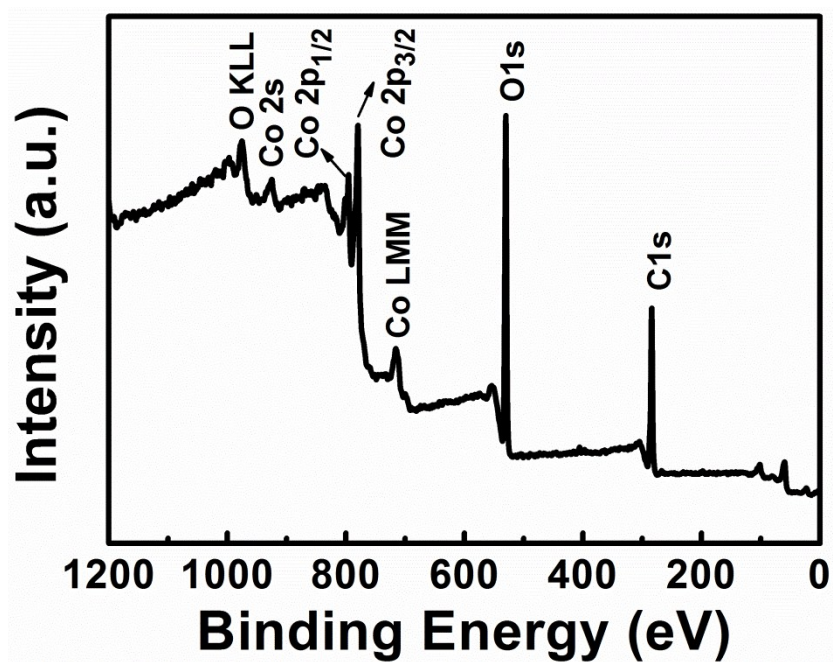


Fig. S5 The XPS spectrum of Co 2D-ICPP.

Table S2 the XRD peaks of Co 2D-ICPP.

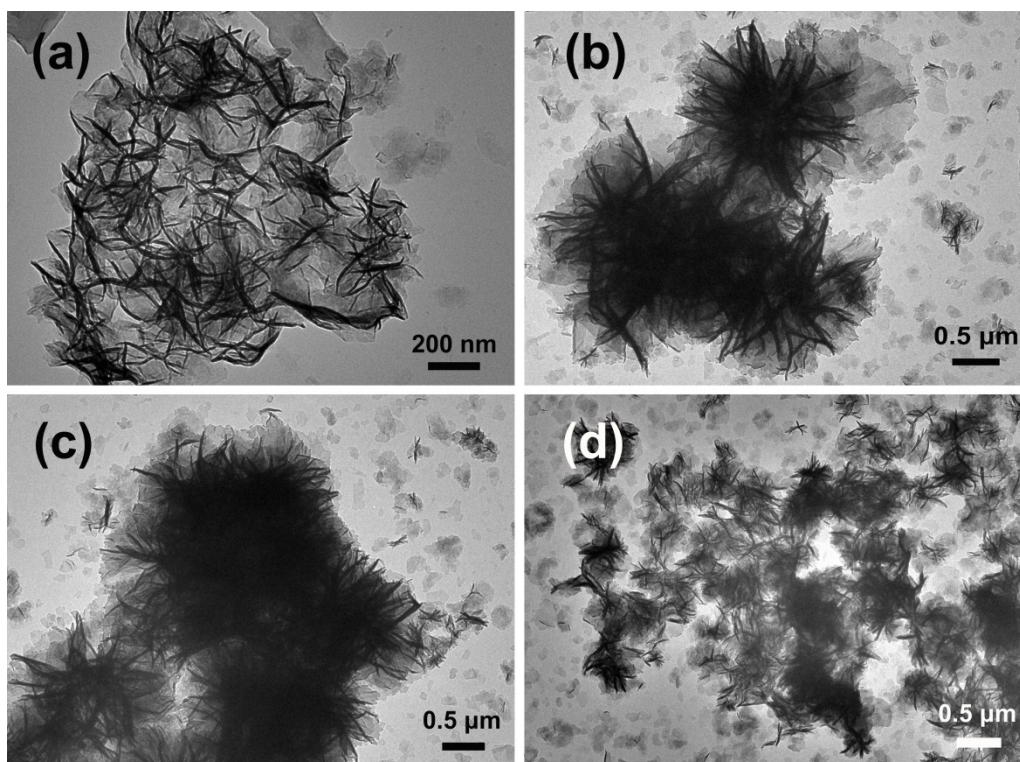
Numbers	(1)	(2)	(3)	(4)	(5)	(6)	(7)	(8)	(9)
2theta(deg)	11.04	22.22	33.44	37.78	44.89	58.18	59.41	65.16	77.3

Table S3 the EA analysis result of Co 2D-ICPP.

Type Value	C	N	H
Calculation(%)	13.12	2.86	3.54
Experiment(%)	13.10	2.81	3.53



### Section 3 The complementary research of self-assemble mechanism.



**Fig. S6** (a) to (d) The TEM images of Co 2D-ICPP in 1 h, 4 h, 7 h and 12 h, respectively.

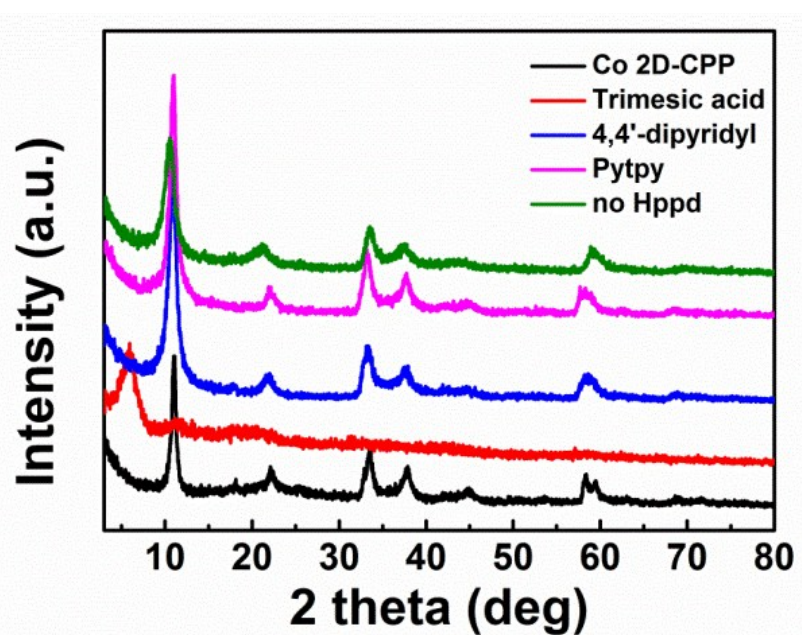


**Fig. S7** The XRD patterns of the products obtained with different modulating agents.

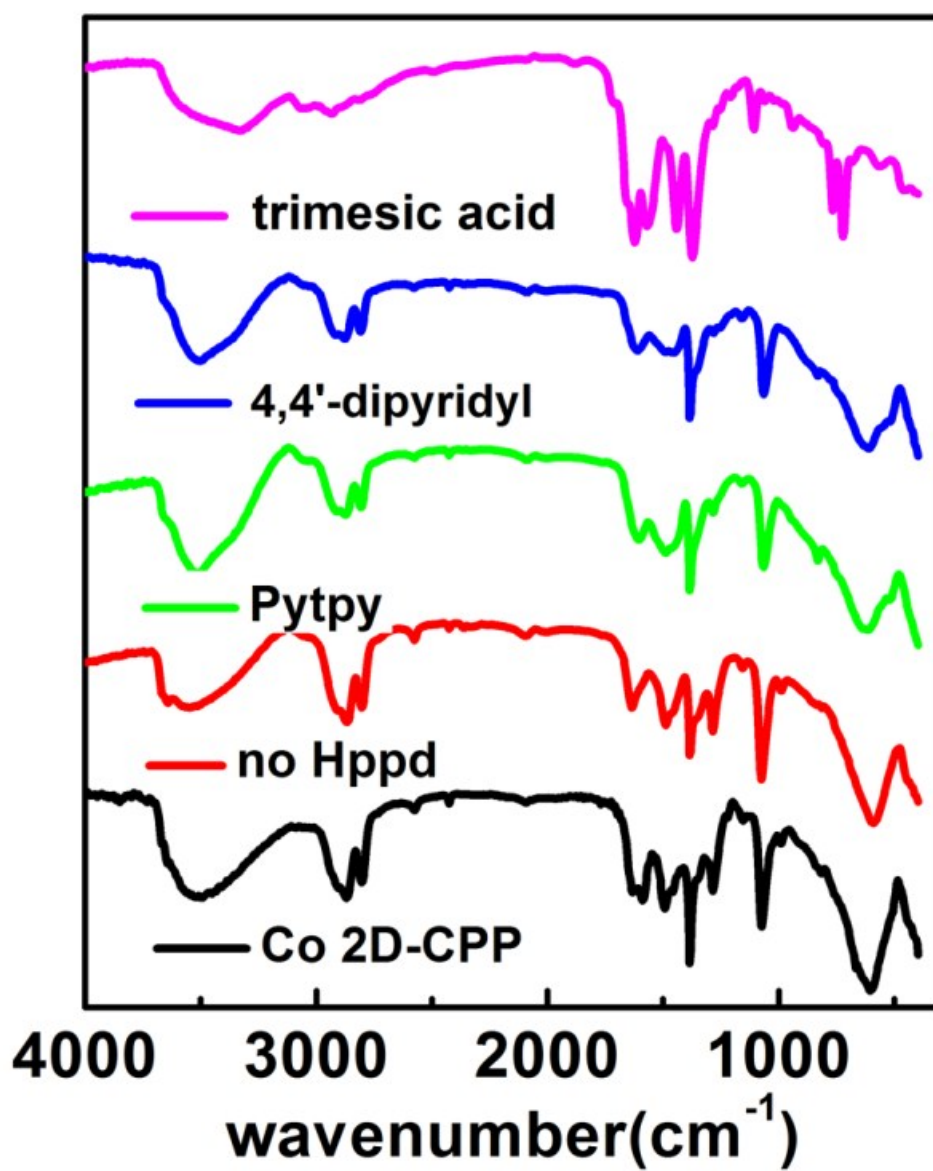


**Fig. S8** The IR spectra of the products obtained with different modulating agents.

Section 4 The supplementary information of Cobalt oxide 2D nano-assemblies,  $\text{Co}_3\text{O}_4/\text{G}$  nanocomposite and Co 2D-ICPP/G nanocomposite.

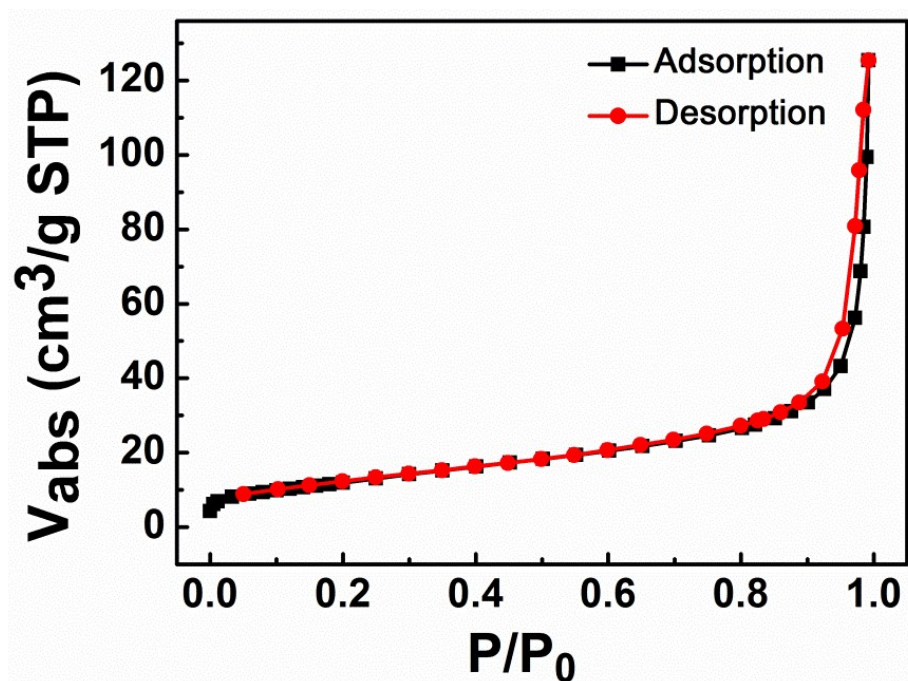
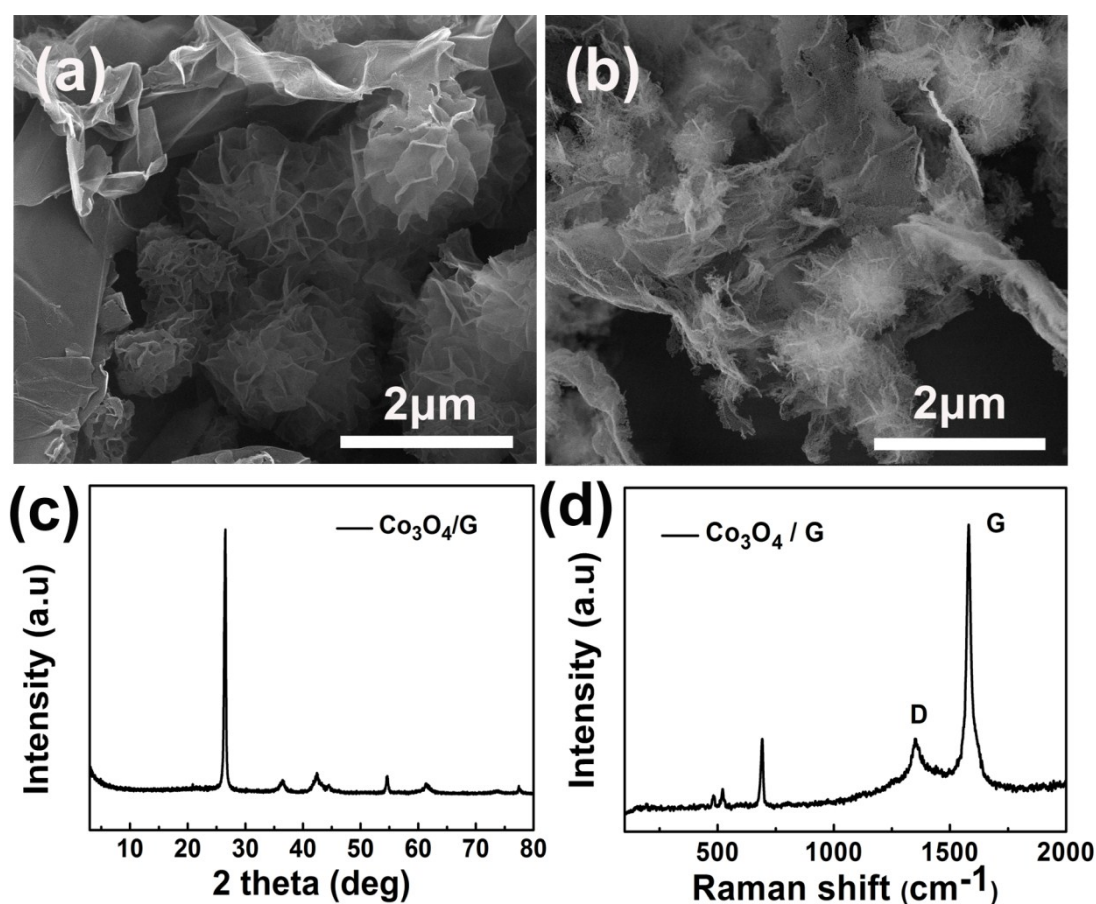


Fig. S9  $\text{N}_2$  adsorption-desorption isotherms of  $\text{Co}_3\text{O}_4$ .



The  $\text{Co}_3\text{O}_4/\text{graphene}$  ( $\text{Co}_3\text{O}_4/\text{G}$ ) nanocomposite can be obtained by the calcination of Co 2D-ICCP/graphene composite precursor. As shown in Fig. S10 (a) and (b), the 2D rose-like assemblies morphology of  $\text{Co}_3\text{O}_4/\text{G}$  can be remained well after calcination. The  $\text{Co}_3\text{O}_4/\text{graphene}$  nanoparticles distribute on the graphene uniformly. The degree of crystallization of the graphene can be relatively determined by the  $I_{\text{D}}/I_{\text{G}}$  ratio in the Raman spectroscopy. The low  $I_{\text{D}}/I_{\text{G}}$  ratio (Fig. S10(d)) corresponds to a high crystallization degree of the  $\text{Co}_3\text{O}_4/\text{G}$  nanocomposite.



**Fig. S10** (a) and (b) The SEM images of  $\text{Co}_3\text{O}_4/\text{G}$  before calcination and after calcination, respectively; (c) The XRD pattern of  $\text{Co}_3\text{O}_4/\text{G}$ ; (d) The Raman spectrogram of  $\text{Co}_3\text{O}_4/\text{G}$ .

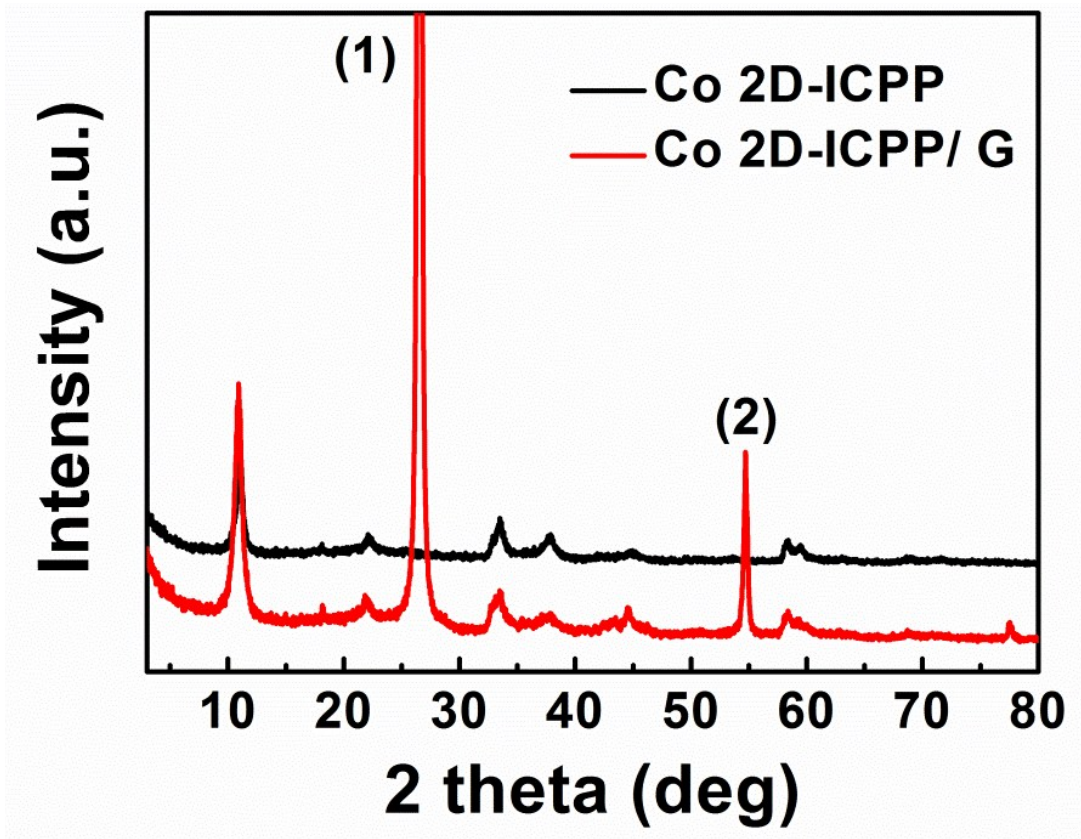


Fig. S11 The XRD patterns of Co 2D-ICPP and Co 2D-ICPP/G.

As the graphene have persistent weight loss when the temperature is increasing,<sup>1,2</sup> we could hardly caculate the weight percent of Co 2D-ICPP from the TGA curve directly. We figure out the Co 2D-ICPP is about 30% via the weight percent of  $\text{Co}_3\text{O}_4$  11.5% in Fig. S12, and the weight percent of graphene is about 70%.

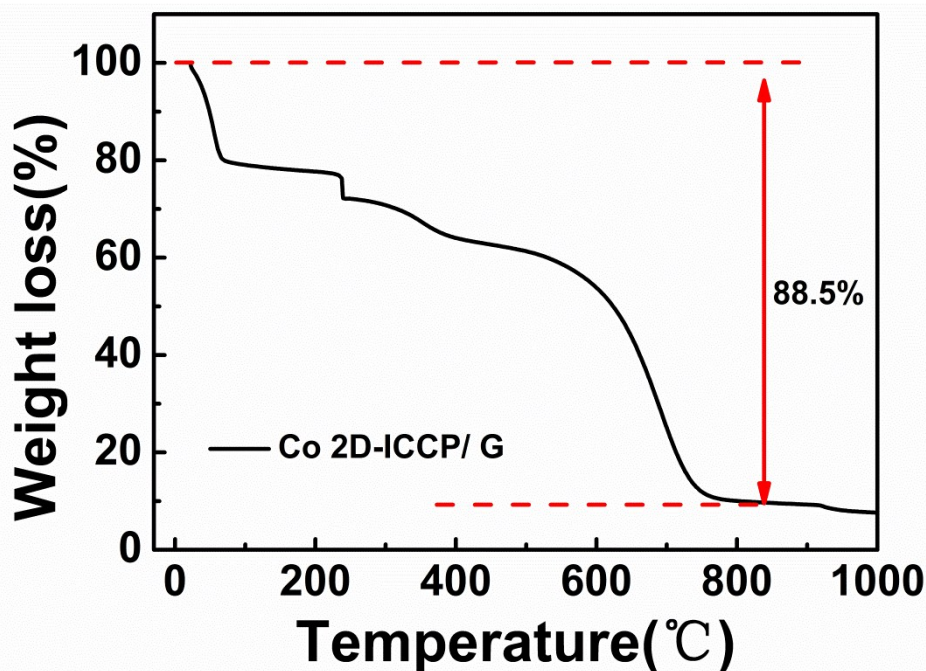


Fig. S12 The TGA curve of Co 2D-ICPP/G.

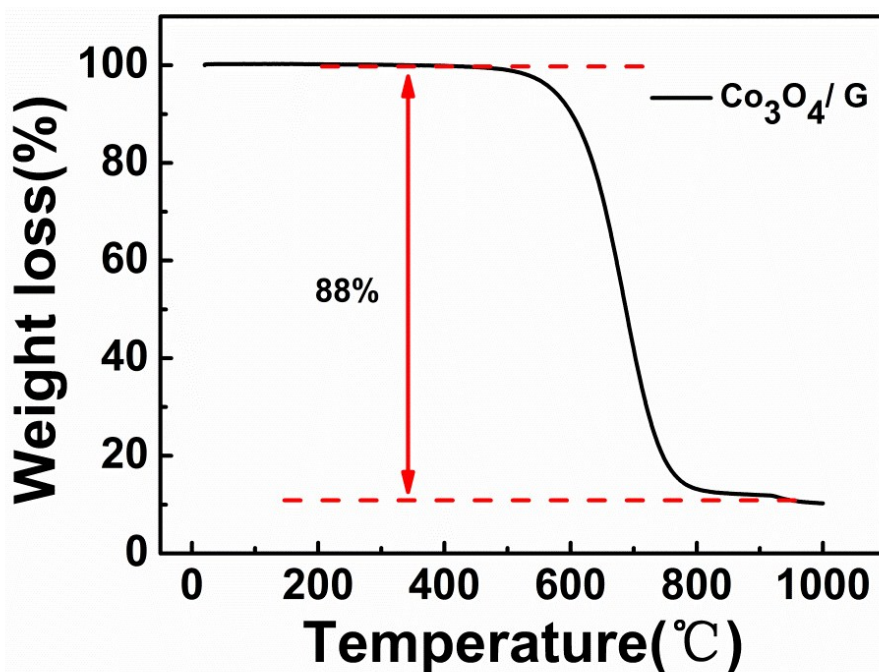


Fig. S13 The TGA curve of  $\text{Co}_3\text{O}_4/\text{G}$ .

Section 5 Cobalt oxide 2D nano-assemblies used as lithium anode material.

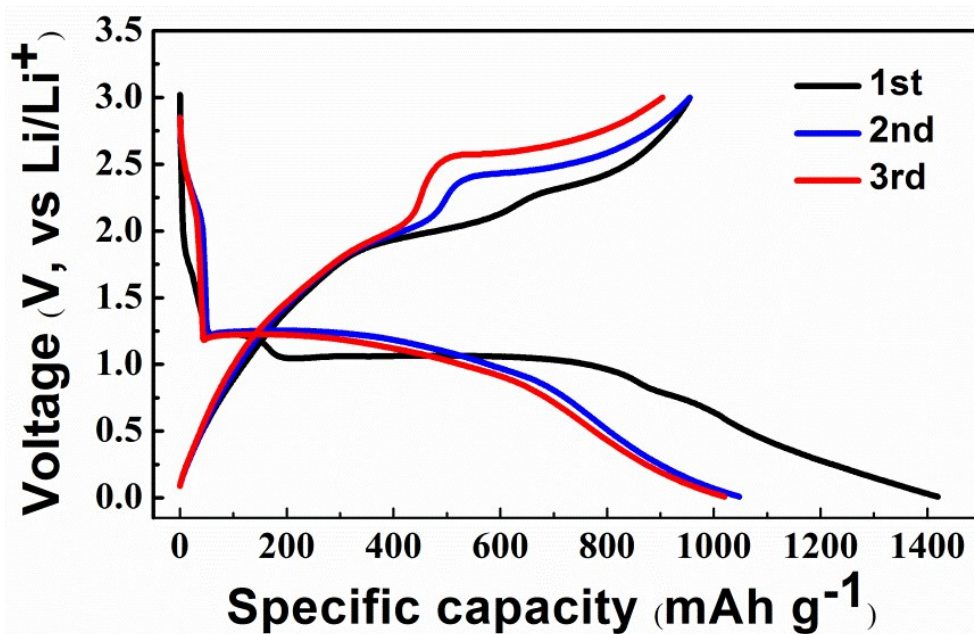
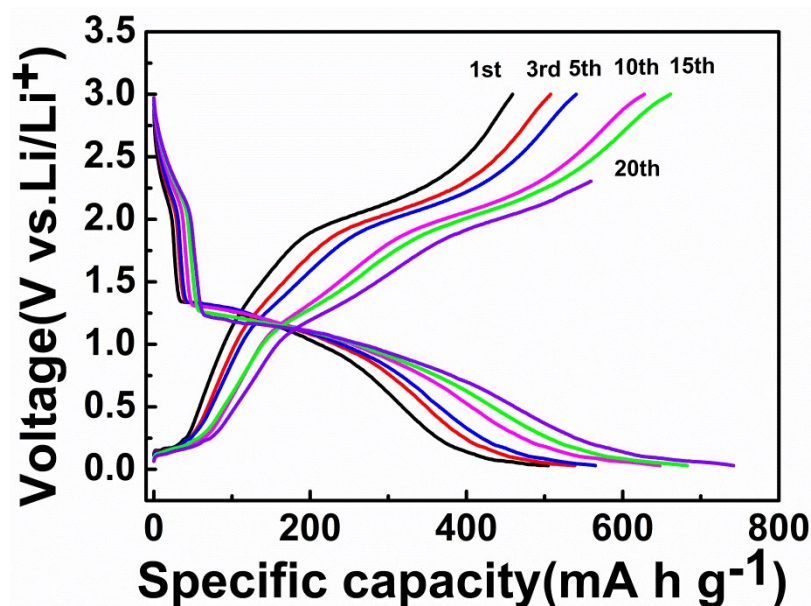


Fig. S14 The charge-discharge voltage profiles of Co<sub>3</sub>O<sub>4</sub> 2D nano-assemblies in the voltage range 0.01-3 V at a current density of 50 mA g<sup>-1</sup>.



**Section 6 Co<sub>3</sub>O<sub>4</sub>/G nanocomposites with other pyridyl modulators used as lithium anode material.**



**Fig. S15** The charge-discharge voltage profiles of Co<sub>3</sub>O<sub>4</sub>/G nanocomposite with 4,4'-dipyridyl as modulator in the voltage range 0.01-3 V at a current density of 50 mA g<sup>-1</sup>.

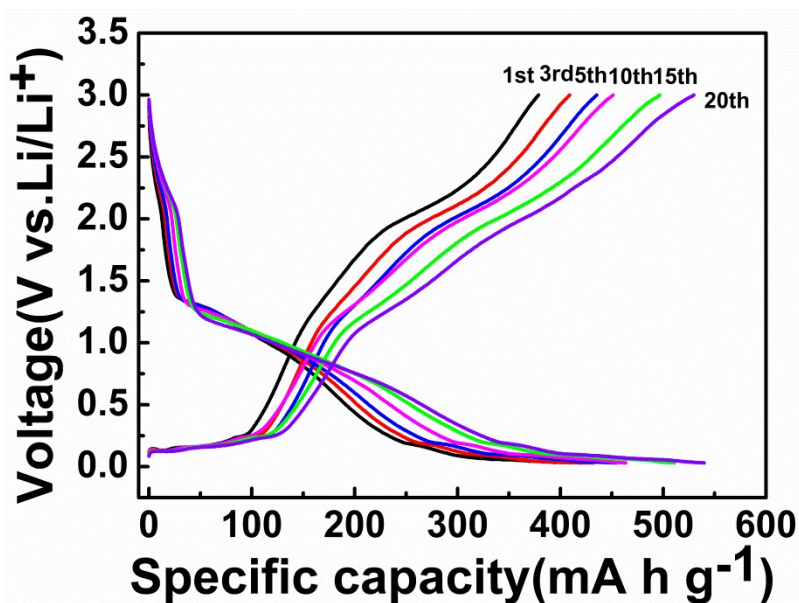


**Fig. S16** The charge-discharge voltage profiles of Co<sub>3</sub>O<sub>4</sub>/G nanocomposite with Pytpy as modulator in the voltage range 0.01-3 V at a current density of 50 mA g<sup>-1</sup>.



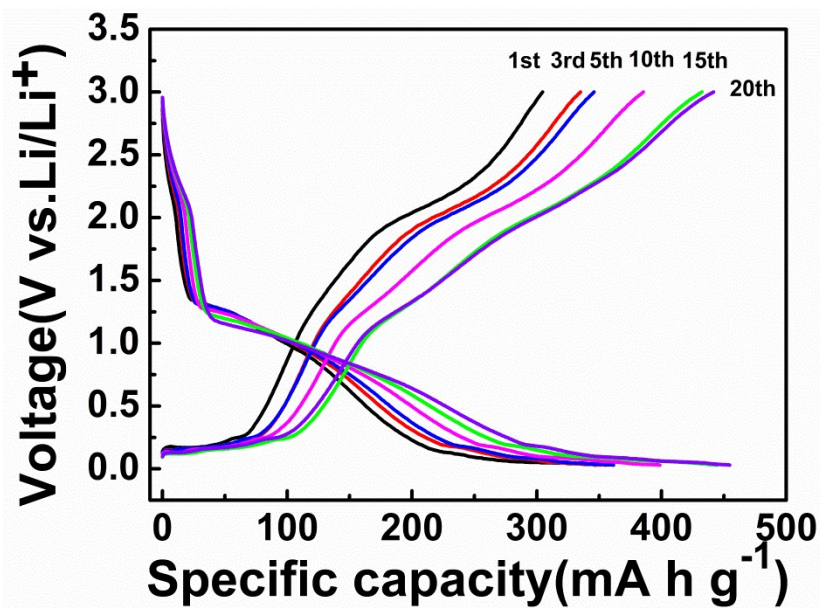


**Fig. S17** The charge-discharge voltage profiles of  $\text{Co}_3\text{O}_4/\text{G}$  nanocomposite with no modulator in the voltage range 0.01-3 V at a current density of  $50 \text{ mA g}^{-1}$ .

## References

1. M. Fang, K. Wang, H. B. Lu, Y. L. Yang, and S. Nuttb, *J. Mater. Chem.*, 2010, **20**, 1982.
2. J. F. Shen, Y. Z. Hu, C. Li, C. Qin, M. Shi, and M. X. Ye, *Langmuir*, 2009, **25**, 6122.